



In vivo and in vitro SAR of tetracyclic MAPKAP-K2 (MK2) inhibitors. Part II

Laszlo Revesz *, Achim Schlapbach, Reiner Aichholz, Janet Dawson, Roland Feifel, Stuart Hawtin, Amanda Littlewood-Evans, Guido Koch, Markus Kroemer, Henrik Möbitz, Clemens Scheufler, Juraj Velcicky, Christine Huppertz

Novartis Institutes for BioMedical Research, CH-4002 Basel, Switzerland

ARTICLE INFO

Article history:

Received 11 March 2010
Revised 7 April 2010
Accepted 7 April 2010
Available online 11 April 2010

Keywords:

MAPKAP-K2
MK2
TNF α
Inhibition
Antiinflammatory
In vivo
Rheumatoid arthritis

ABSTRACT

Spirocyclopropane- and spiroazetidine-substituted tetracycles **13D–E** and **16A** are described as orally active MK2 inhibitors. The spiroazetidine derivatives are potent MK2 inhibitors with $IC_{50} < 3$ nM and inhibit the release of TNF α ($IC_{50} < 0.3$ μ M) from hPBMCs and hsp27 phosphorylation in anisomycin stimulated THP-1 cells. The spirocyclopropane analogues are less potent against MK2 ($IC_{50} = 0.05$ – 0.23 μ M), less potent in cells ($IC_{50} < 1.1$ μ M), but show good oral absorption. Compound **13E** (100 mg/kg po; bid) showed oral activity in rAIA and mCIA, with significant reduction of swelling and histological score.

© 2010 Elsevier Ltd. All rights reserved.

Mitogen-activated protein kinases (MAPKs) belong to the Ser/Thr kinase family¹, control cytoskeletal architecture, cell-cycle progression and are implicated in inflammation and cancer.² The p38/MAPKAP kinase-2 (MAPKAP-K2; MK2) cascade plays a pivotal role in the production of proinflammatory cytokines, such as TNF α , IL-6 and IFN γ .³ Moreover, MK2 knock-out mice are resistant to developing disease in arthritis models.⁴ Thus, MK2 has emerged as a highly desirable target in the search for efficacious and safe anti-inflammatory drugs. MK2 inhibitors from a variety of structural classes were published, including aminocyanopyridines, tetrahydro- γ -carbolines and pyrrolopyridines, pyrrolo-pyrimidinones, benzothiophenes, 2,4-diamino-pyrimidines⁵ and 3-aminopyrazoles.⁶ A breakthrough with low-molecular MK2-inhibitors is still awaited.⁷

Our screening efforts for MK2 inhibitors identified the pyrrolo[2,3-*f*]isoquinoline amide **1** (Fig. 1) as a modest MK2 inhibitor with an IC_{50} value of 3.8 μ M. **1** demonstrated structural similarities to the recently disclosed MK2 inhibitors **2**^{5g} with a pyrrolopyridine scaffold and submicromolar IC_{50} . Combining the structural features of **1** and **2** resulted in the tetracyclic MK2 inhibitor **3**⁸ with an IC_{50} of 10 nM. In spite of potent cellular activity, **3** was lacking oral bioavailability. Here we report our efforts towards orally active MK2 inhibitors by modifying the tetracyclic $\alpha\beta\gamma\delta$ -ring system of **4**.

Pyrrole-tetracycles **4a** (Scheme 1) were prepared via the Hantzsch⁹ reaction of bromoketone **5** and piperidinedione **6** followed by Suzuki coupling¹⁰ with R¹-substituents **A–F**. Furan-tetracycles **4b** with a furan as γ -ring (Scheme 1) were obtained in a similar fashion, first by reacting **5** and **6** to a 1,4-diketone intermediate which was then cyclised to the furan-ring in the presence of H₂SO₄.

Desired bromoketones **5a–c** (Scheme 2) were prepared in eight steps¹¹ from cyclopentanone, cyclohexanone and cycloheptanone. Bromoketone **5d** was gained from 2-ethoxycarbonyl cyclohexanone in six steps.¹¹ Piperidinediones **6** were synthesized starting from β -aminoesters **9a–f** by their reaction with mono-chloromalonate, followed by Dieckmann condensation (MeONa in refluxing

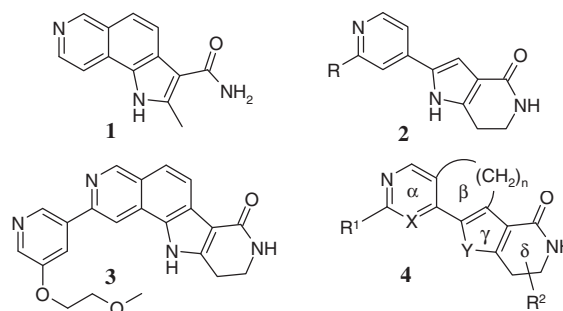
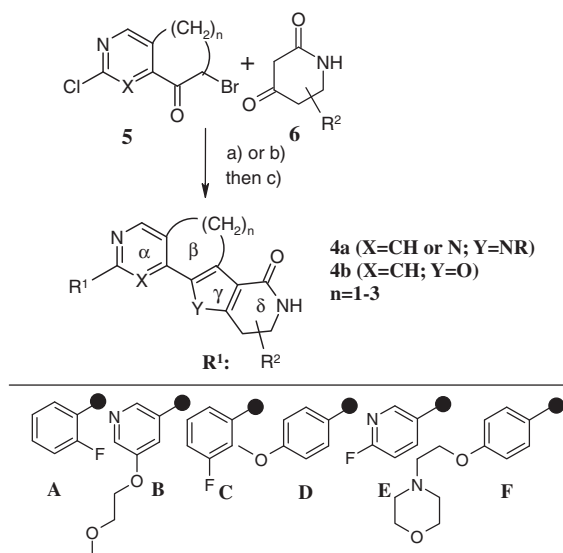


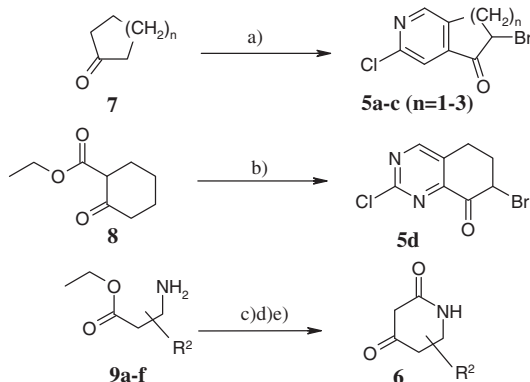
Figure 1. MK2 inhibitors.

* Corresponding author. Fax: +41 61 324 3273.

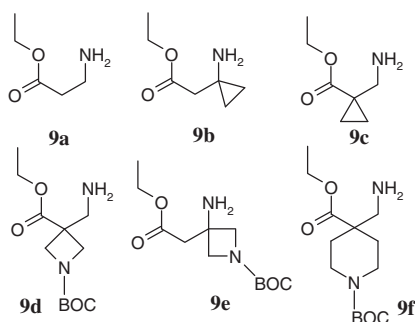
E-mail address: laszlo.revesz@pharma.novartis.com (L. Revesz).



Scheme 1. Reagents and conditions: (a) MeOH, NH_4OAc , rt, 12 h, 25–60% of **4a** ($\text{R}^1 = \text{Cl}$; $\text{X} = \text{CH}$ or N); (b) (i) MeOH, NaOAc , 12 h, rt, then evaporate, (ii) $\text{H}_2\text{SO}_{4\text{conc}}$, rt, 10 min., 23–55% of **4b** ($\text{R}^1 = \text{Cl}$; $\text{X} = \text{CH}$); (c) $\text{R}^1\text{-B(OH)}_2$ or its pinacol ester, $\text{Pd}(\text{PPh}_3)_2\text{Cl}_2$, PPh_3 , 2 N Na_2CO_3 , 1-propanol, 150 °C, 20 min., microwave, 60–80%.



Scheme 2. Reagents and conditions: (a) eight; (b) six steps as described¹¹; (c) ethyl malonyl chloride, NEt_3 , CH_2Cl_2 , rt, 30 min, 40–60%; (d) MeONa , toluene, reflux 45 min., quant; (e) $\text{MeCN}/\text{H}_2\text{O}$ reflux, 1 h, 85%.

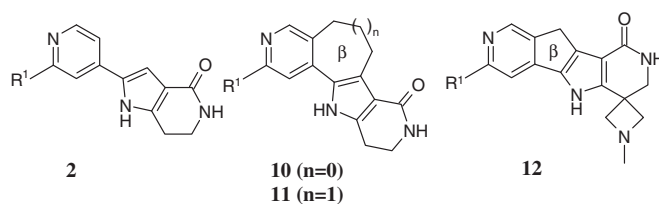


Scheme 3. 3-Amino propionic acid ethyl esters.

toluene) of the obtained amides and decarboxylation in refluxing wet acetonitrile.¹¹

β -Aminoesters **9a–c** and **9f** are commercially available, while derivatives **9d–e** are novel and were prepared as described previously¹¹ (Scheme 3).

Regarding MK2-inhibition and cellular activity, the conformationally restricted tetracycles **10** and **11** (Scheme 4) proved to be



Scheme 4. Conformationally restricted MK2 inhibitors **10–12**.

Table 1
Conformationally restricted MK2 inhibitors **10–12**

Compd	MK2 ^a (M)	TNF α ^b (μM)	<i>p</i> -hsp27 ^c (μM)	Sol. ^d (μM)
2A	0.560	>10	8.9	337
3	0.010	0.3	1.5	<4
10A	0.037	1.5	2.7	11
10B	0.040	0.4	1.7	8
11B	0.180	1.1	4.3	21
12A	0.230	>10	10.0	69

^a IC_{50} values are measured as described⁶ and are reported as a mean of ≥ 2 measurements with a standard deviation of less than $\pm 50\%$.

^b Inhibition of LPS stimulated release of TNF α from hPBMC is performed as described.⁶

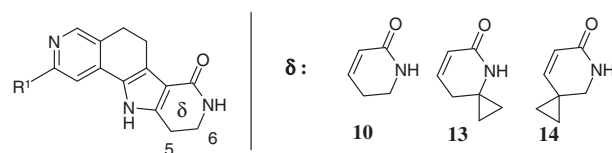
^c Inhibition of anisomycin stimulated phosphorylation of hsp27 in THP-1 cells is measured as described.⁶

^d Thermodynamic solubility measured at pH 6.8.

clearly superior to the non-cyclised pyrrolopyridines **2** (Table 1). Thus, a comparison of **2A**^{5g} with **10A** revealed that the former was a weak MK2 inhibitor devoid of cellular activity in contrast to its cyclised analogue **10A**, which was 15-times more potent against MK2 and inhibited LPS-induced release of TNF α from hPBMCs and hsp27 phosphorylation with low micromolar IC_{50} s. Compound **10B** was slightly less potent than its fully aromatic analogue **3**, but with improved solubility (8 μM vs <4 μM). Ring expansion of **10B** to **11B** with a seven-membered β -ring resulted in ~ 3 -fold lower MK2- and cellular potency. Ring contraction of **10B** to a five-membered β -ring yielded **12A** again with lower MK2-affinity ($\text{IC}_{50} = 0.23 \mu\text{M}$) lacking cellular activity.

Keeping the six-membered β -ring unchanged, the influence of three- and four-membered spirocycles attached to the lactam δ -ring was investigated (Scheme 5, Table 2). Spirocyclopropanes **13**, **14** and the unsubstituted analogue **10** showed similar MK2- and cellular inhibition profiles. IC_{50} for MK2 inhibition was in the range of 8 nM (**10C**) to 0.23 μM (**13C**), the IC_{50} for inhibition of TNF α from hPBMCs in the range of 0.1 μM (**10D**) to 1.7 μM (**14D**). Intracellular *p*-hsp27 was inhibited at a slightly higher range from $\text{IC}_{50} = 0.5 \mu\text{M}$ (**13C**) to 2.7 μM (**10A**). Solubilities were modest, best values reaching 10–11 μM at pH 6.8 (**10A** and **13A**). Whereas R^1 -substituents **A–F** had no major effect on kinase affinity or cellular potency, the *o*-fluorophenyl substituent **A** had a favourable effect on solubility. Solubilising groups **B** and **F** failed to enhance solubilities probably due to the rigid flat tetracyclic core leading to a tight crystal packing.

MK2 inhibition and cellular potency of the spiroazetidines (Scheme 6, Table 3) appeared to depend upon their position on the δ -ring.

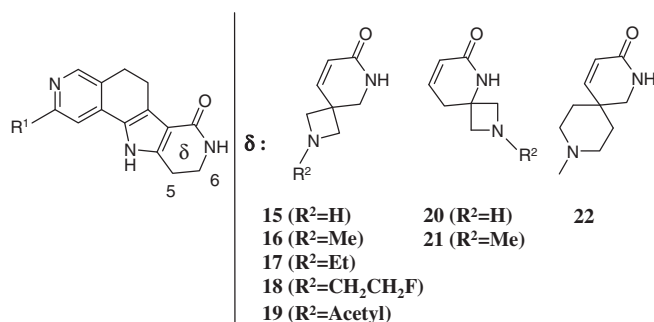


Scheme 5. δ -Ring modifications.

Table 2
δ-Ring modifications

Compd	MK2 ^a (μM)	TNFα ^b (μM)	<i>p</i> -hsp27 ^a (μM)	Sol. ^d (μM)
10C	0.008	0.5	1.3	<4
10D	0.080	0.1	0.7	<4
13A	0.140	0.9	0.7	10
13C	0.230	0.8	0.5	5
13D	0.175	0.2	0.7	<4
13E	0.050	0.3	1.1	9
13F	0.100	0.2	1.4	<4
14C	0.100	0.9	0.9	<4
14D	0.130	1.7	1.2	<4
14E	0.027	0.7	1.4	<4

a–d See Table 1.

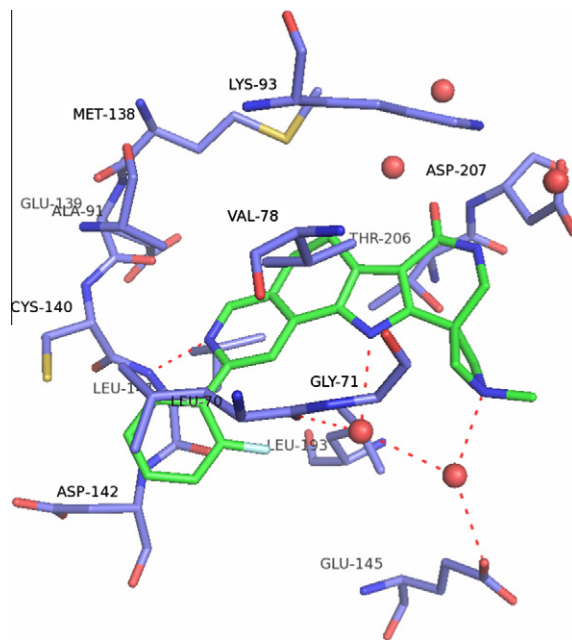
**Table 3**
δ-Ring modifications

Compd	MK2 ^a (μM)	TNFα ^b (μM)	<i>p</i> -hsp27 ^c (μM)	Sol. ^d (μM)
15A	0.017	0.1	0.1	337
15C	<0.003	0.2	0.2	n.t.
16A	<0.003	0.1	0.3	>1000
16B	<0.003	0.7	1.4	n.t.
16C	<0.003	0.2	0.2	10
16D	<0.003	0.06	0.7	40
16E	<0.003	0.1	1.2	47
16F	<0.003	0.6	1.2	n.t.
17A	<0.003	0.7	1.5	950
18A	0.230	1.5	6.5	n.t.
19A	0.12	6.5	25	24
20D	0.012	1.3	3.1	32
21D	0.045	1.1	17.0	<4
22A	0.004	0.2	0.7	>1000

a–d See Table 1. n.t.: not tested.

Spiroazetidines at the 5-position (**15–17**) were highly potent, while their analogues at the 6-position (**20 and 21**) were considerably weaker, especially after azetidine *N*-methylation, exemplified by **21D** with a dramatic loss of cellular activity in the *p*-hsp27 assay ($IC_{50} = 17 \mu M$). The inhibition of TNFα by **21D** ($IC_{50} = 1.1 \mu M$) may result from an off-target effect. Azetidines **16A–F** and **17A** with their *N*-methyl and *N*-ethyl groups pointing into the sugar pocket belong to the most potent MK2-inhibitors presented here, all with $IC_{50} = <0.003 \mu M$, independent of R¹. An explanation for their high affinity is offered by the crystal structure of **16A**, which reveals a water mediated interaction between the basic azetidine nitrogen of this ligand and the carboxylic residue Glu-145 of MK2 (Fig. 2).

These derivatives exhibit also a potent inhibition of TNFα in hPBMCs ranging from $IC_{50} = 0.06 \mu M$ (**16D**) to $0.7 \mu M$ (**17A and 16B**), inhibition of *p*-hsp27 was in the range of $IC_{50} = 0.2 \mu M$ (**16C**) to $1.5 \mu M$ (**17A**). *N*-Fluoroethyl (**18A**) and *N*-acetyl (**19A**) showed a dramatic decrease in MK2- and cellular activity, thus

**Figure 2.** Crystal structure of **16A** bound to MK2.¹²

demonstrating the importance of a basic nitrogen at this position. Interestingly, the *o*-fluorophenyl substituent **A** had again a pronounced influence on solubility, possibly due to a slight out-of-plane rotation (see X-ray analysis, Fig. 2). While solubilities of **16C–E** reached in the best case $47 \mu M$ (**16E**), at pH 6.8, piperidine **22A** and azetidine **16A** with *o*-fluorophenyl substituents reached solubilities of $>1000 \mu M$. Compound **22A** was slightly less potent in cells (TNFα $IC_{50} = 0.2 \mu M$; *p*-hsp27 = $0.7 \mu M$) and against MK2 ($IC_{50} = 4 \text{ nM}$).

Substituting pyridine by pyrimidine in the α-ring of the tetracyclic core led to the series **23–26** (Scheme 7, Table 4).

Pyrimidines **23–26** were found to be weaker than their pyridine analogues **10** and **13–15**. Spiroazetidines in this series were again more potent than spirocyclopropanes; spiroazetidines **26A–F** inhibited MK2 with potencies ranging from $IC_{50} < 0.003 \mu M$ (**26D and 26F**) to $IC_{50} = 0.034 \mu M$ (**26A**). Unfortunately, the cellular efficacies did not reach the level of the pyridine analogues; the most potent compound in terms of *p*-hsp27 inhibition was spiroazetidine **26E** ($IC_{50} = 1.8 \mu M$).

Further, we also explored the γ-ring of the tetracyclic core by replacement of the pyrrole in **15C** and **16C** by furan leading to derivatives **27** and **28** (Scheme 8, Table 5). Compound **27** showed weak MK2-affinity ($IC_{50} = 0.2 \mu M$) and proved to be 10–100-fold weaker in cells compared to its pyrrole-NH analogue **15C**. Corresponding *N*-methyl azetidine **28** was even weaker (1000-fold) against MK2 than its pyrrole-NH analogue **16C**. To investigate the importance of the pyrrole-NH for the MK2-binding, pyrrole-NME derivatives **29** and **30** were prepared and tested. Interestingly, a less dramatic drop in activity was observed in comparison to the furan analogues: **29** and **30** still showed some cellular efficacies.

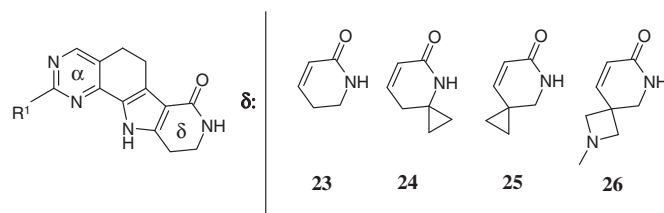
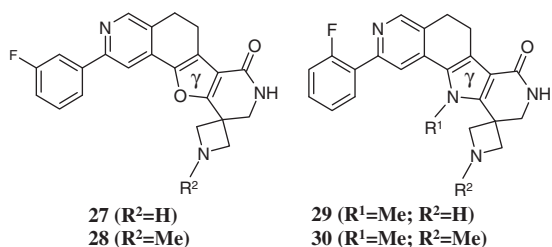


Table 4
Pyrimidines

Compd	MK2 ^a (μM)	TNF α ^b (μM)	<i>p</i> -hsp27 ^c (μM)	Sol. ^d (μM)
23D	0.270	0.9	4.3	<5
24A	0.860	2.3	15.3	8
24D	0.900	nt	2.5	<4
24E	0.120	0.7	12.0	<4
24F	0.180	0.3	3.2	<4
25D	0.150	0.4	5.6	<4
26A	0.034	1.6	5.6	373
26B	0.006	1.5	6.7	n.t.
26C	0.006	0.5	4.5	n.t.
26D	<0.003	0.1	3.0	43
26E	0.007	0.7	1.8	173
26F	<0.003	0.1	2.8	n.t.

^{a-d} See Table 1. n.t.: not tested.**Scheme 8.** γ -Ring modifications.**Table 5**
 γ -Ring modifications

Compd	MK2 ^a (μM)	TNF α ^b (μM)	<i>p</i> -hsp27 ^c (μM)	Sol. ^d (μM)
27	0.200	2.5	17	51
28	3.300	n.t.	n.t.	n.t.
29	0.020	1.8	1.3	54
30	0.013	1.1	1.7	41

^{a-d} See Table 1. n.t.: not tested.

Selected compounds were tested in the LPS-induced TNF α release model in mice¹³ at 100 mg/kg po (Table 6). Unfortunately, none of the in vitro highly potent azetidine-NH analogues **15** showed any oral efficacy (not shown in Table 6). Among the *N*-methyl azetidine analogues only **16A** showed good oral activity, while none of the other R¹-substituents **C–E** was able to confer oral efficacy within the **16**-scaffold. The spirocyclopropanes **13** and **14**—indistinguishable in vitro—demonstrated big differences in vivo, where only the series **13** yielded good oral efficacies. Compounds **13D** and **13E** inhibited 81% and 96% of TNF α release in mice at 25 μM and 30 μM plasma concentrations. Their isomers **14D** and **14E** inhibited only 16% and 30% of TNF α at 0.6 μM and 1.9 μM plasma exposures. Interestingly, the highly soluble **16A**

Table 6
TNF α inhibition in LPS-treated mice

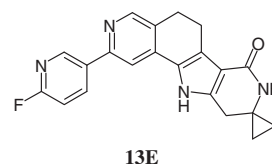
Compd	%TNF α inhibition ^a	Plasma exposure (μM)
13C	55	15
13D	81	25
13E	96	30
14D	16	0.6
14E	30	1.9
16A	90	6
16C	0	1
16D	0	0.1
16E	26	0.6

^a MK2-inhibitors were administered at a dose of 100 mg/kg po.¹³

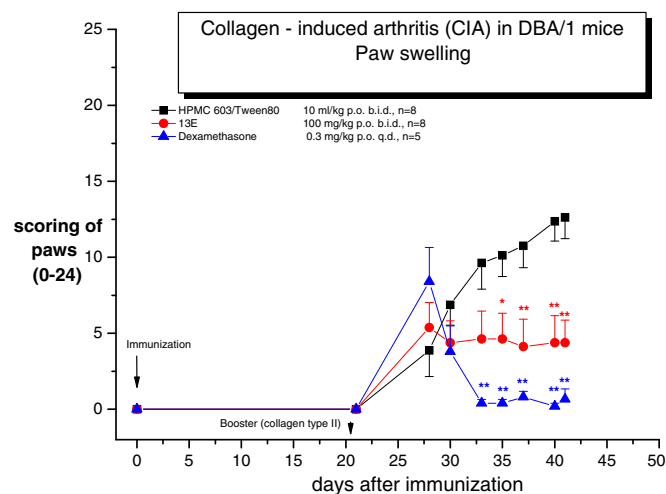
shows lower exposure levels than the less soluble **13D** and **13E**. This is no contradiction, since the thermodynamic solubilities measured at pH 6.8 do not predict oral exposures which depend upon further additional parameters.

Good pharmacokinetic properties of compound **13E** in rats (1 mg/kg po; *F*: 24%; *C*_{max}: 105 nM; clearance: 12 mL min⁻¹ kg⁻¹; *V*_{ss}: 1.9 L kg⁻¹; AUC: 2000 nmol h L⁻¹; *t*_{1/2}: 1.3 h) permitted this compound to be tested in chronic models of rheumatoid arthritis in mice and rats. In the collagen-induced arthritis in DBA/1 mice¹⁴ (100 mg/kg po bid) **13E** significantly reduced swelling and histological scores (Fig. 3) (joint damage and erosions, proteoglycan loss and inflammatory cell infiltrates).

Similarly, **13E** (100 mg/kg po bid) reduced swelling in the rat antigen-induced arthritis¹⁵ (rAIA) model (Fig. 4). In addition, **13E** was well tolerated; no body weight reduction compared to vehicle treatment was observed. Blood samples taken 2, 6 and 16 h after the last dosing revealed good exposure of **13E** in both models: 16, 2.4 and 0 μM (in mCIA) and 11.7, 9.8 and 0.5 μM (in rAIA). Due to the high plasma concentrations it can not be ruled out, that the effects seen in chronic models may not be the result of MK2-inhibition alone, but may also be attributed to the inhibition of other kinases.¹⁶

**13E**

In summary, our SAR studies have led to the discovery of two orally active MK2 inhibitor series: the spirocyclopropanes **13C–E** and the spiroazetidine **16A**. The spiroazetidines belong to the most potent MK2 inhibitors known to date with IC₅₀ <3 nM and show high cellular potencies (IC₅₀ <0.3 μM) in inhibiting TNF α release from LPS challenged hPBMCs as well as in inhibiting hsp27 phosphorylation in THP-1 cells, while they generally suffer from low oral absorption and high clearance. Spirocyclopropanes on the other hand are less potent against MK2 (IC₅₀ = 0.05–0.23 μM) and in cells (IC₅₀ <1.1 μM), but they display better absorption and moderate clearance in vivo. Selected compound **13E** showed oral activity in rAIA and mCIA at 100 mg/kg po bid, by significantly reducing swelling and histological scores.

**Figure 3.** Inhibition of mCIA by **13E**.¹⁴

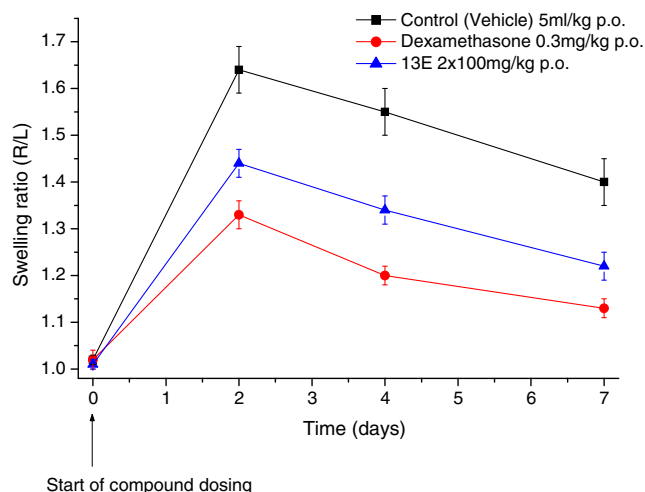


Figure 4. Inhibition of rAIA by 13E.¹⁵

Acknowledgements

The kilolab is gratefully acknowledged for preparing ample quantities of 4-aza-spiro-[2.5]octane-5,7-dione, 7,9-dioxo-2,6-diaza-spiro-[3.5]nonane-2-carboxylic acid *tert*-butyl ester and 3-chloro-7,8-dihydro-6*H*-isoquinolin-5-one. We thank Dr. Karl Welzenbach for technical assistance in measuring phosphorylation of hsp27 using flow cytometry.

References and notes

- Chen, Z.; Gibson, T. B.; Robinson, F.; Silvestro, L.; Pearson, G.; Xu, B.; Wright, A.; Vanderbilt, C.; Cobb, M. H. *Chem. Rev.* **2001**, *101*, 2449.
- Gaestel, M. *Nat. Rev. Mol. Cell Biol.* **2006**, *7*, 120.
- Kotlyarov, A.; Yannoni, Y.; Fritz, S.; Laass, K.; Telliez, J. B.; Pitman, D.; Lin, L. L.; Gaestel, M. *Mol. Cell Biol.* **2002**, *22*, 4827.
- Hegen, M.; Gaestel, M.; Nickerson-Nutter, C. L.; Lin, L.-L.; Telliez, J.-B. *J. Immunol.* **2006**, *177*, 1913.
- (a) Schlapbach, A.; Feifel, R.; Hawtin, S.; Heng, R.; Koch, G.; Moebitz, H.; Revesz, L.; Scheuffler, C.; Velcicky, J.; Waelchli, R.; Huppertz, C. *Bioorg. Med. Chem. Lett.* **2008**, *18*, 6142; (b) Anderson, D. R.; Hegde, S.; Reinhard, E.; Gomez, L.; Vernier, W. F.; Lee, L.; Liu, S.; Sambandam, A.; Snider, P. A.; Masih, L. *Bioorg. Med. Chem. Lett.* **2005**, *15*, 1587; (c) Wu, J.-P.; Wang, J.; Abeywardane, A.; Andersen, D.; Emmanuel, M.; Gautschi, E.; Goldberg, D. R.; Kashem, M. A.; Lukas, S.; Mao, W.; Martin, L.; Morwick, T.; Moss, N.; Pargellis, C.; Patel, U. R.; Patnaude, L.; Peet, G. W.; Skow, D.; Snow, R. J.; Ward, Y.; Werneburg, B.; White, A. *Bioorg. Med. Chem. Lett.* **2007**, *17*, 4664; (d) Trujillo, J. I.; Meyers, M. J.; Anderson, D. R.; Hegde, S.; Mahoney, M. W.; Vernier, W. F.; Buchler, I. P.; Wu, K. K.; Yang, S.; Hartmann, S. J.; Reitz, D. B. *Bioorg. Med. Chem. Lett.* **2007**, *17*, 4657; (e) Goldberg, D. R.; Choi, Y.; Cogan, D.; Corson, M.; DeLeon, R.; Gao, A.; Gruenbaum, L.; Hao, M. H.; Joseph, D.; Kashem, M. A.; Miller, C.; Moss, N.; Netherton, M. R.; Pargellis, C. P.; Pelletier, J.; Sellati, R.; Skow, D.; Torcellini, C.; Tseng, Y.-C.; Wang, J.; Wasti, R.; Werneburg, B.; Wu, J. P.; Xiong, Z. *Bioorg. Med. Chem. Lett.* **2008**, *18*, 938; (f) Xiong, Z.; Gao, D. A.; Cogan, D. A.; Goldberg, D. R.; Hao, M.-H.; Moss, N.; Pack, E.; Pargellis, C.; Skow, D.; Trieselmann, T.; Werneburg, B.; White, A. *Bioorg. Med. Chem. Lett.* **2008**, *18*, 1994; (g) Anderson, D. R.; Meyers, M. J.; Vernier, W. F.; Mahoney, M. W.; Kurumbail, R. G.; Caspers, N.; Poda, G. I.; Schindler, J. F.; Reitz, D. B.; Mourey, R. J. *J. Med. Chem.* **2007**, *50*, 2647; (h) Lin, S.; Lombardo, M.; Malkani, S.; Hale, J. J.; Mills, S. G.; Chapman, K.; Thompson, J. E.; Zhang, W. X.; Wang, R.; Cubbon, R. M.; O'Neill, E. A.; Luell, S.; Carballo-Jane, E.; Yang, L. *Bioorg. Med. Chem. Lett.* **2009**, *19*, 3238; (i) Anderson, D. R.; Meyers, M. J.; Kurumbail, R. G.; Caspers, N.; Poda, G. I.; Long, S. A.; Pierce, B. S.; Mahoney, M. W.; Mourey, R. J. *Bioorg. Med. Chem. Lett.* **2009**, *19*, 4878; (j) Anderson, D. R.; Meyers, M. J.; Kurumbail, R. G.; Caspers, N.; Poda, G. I.; Long, S. A.; Pierce, B. S.; Mahoney, M. W.; Mourey, R. J.; Parikh, M. D. *Bioorg. Med. Chem. Lett.* **2009**, *19*, 4882; (k) Harris, C. M.; Ericsson, A. M.; Argiriadi, M. A.; Barberis, C.; Borhani, D. W.; Burchat, A.; Calderwood, D. J.; Cunha, G. A.; Dixon, R. W.; Frank, K. E.; Johnson, E. F.; Kamens, J.; Kwak, S.; Li, B.; Mullen, K. D.; Perron, D. C.; Wang, L.; Wishart, N.; Wu, X.; Zhang, X.; Zmetra, T. R.; Talanian, R. V. *Bioorg. Med. Chem. Lett.* **2010**, *20*, 334.
- Velcicky, J.; Feifel, R.; Hawtin, S.; Heng, R.; Huppertz, C.; Koch, G.; Kroemer, M.; Moebitz, H.; Revesz, L.; Scheuffler, C.; Schlapbach, A. *Bioorg. Med. Chem. Lett.* **2010**, *20*, 1293.
- Schlapbach, A.; Huppertz, C. *Future Med. Chem.* **2009**, *1*, 1243–1257.
- Revesz, L.; Schlapbach, A.; Waelchli, R. WO 2008025512; *Chem. Abstr.* **2008**, *148*, 331658.
- Elderfield, R.; Dodd, T. N. *Heterocycl. Compd.* **1950**, *1*, 132.
- Suzuki, A. *Pure Appl. Chem.* **1991**, *63*, 419.
- Schlapbach, A.; Revesz, L.; Koch, G. WO 2009010488; *Chem. Abstr.* **2009**, *150*, 168327.
- The X-ray coordinates are deposited with RCSB Protein Data Bank, deposition code is 3M2W. The protein used in this study is a segment of MK2 containing residues 47–364(216–237)G.
- MK2-inhibitors (100 mg/kg p.o.) were administered to OF1 mice (female, 8 weeks old), followed by LPS injection (20 mg/kg) 1 h later. One hour post LPS injection the experiment was terminated and blood withdrawn. Compound blood levels were determined by LC-MS/MS and plasma levels of mouse TNF α determined by ELISA.
- Mouse CIA: Male DBA/1 mice (Janvier 10–12 weeks of age, were immunized with bovine collagen type II in CFA intradermally at the base of the tail. A second injection of bovine collagen type II in PBS was given ip on day 21. Upon initiation of swelling, mice were randomized into groups of 8 (test substance and vehicle) or 5 (steroid positive control) and treated with 13E, vehicle or dexamethasone from day 28 to day 41.
- Rat AIA: Arthritis was induced in the right knee of rats by intra-articular injection of methylated bovine serum albumin (mBSA), in animals previously sensitised to the same antigen. Treatment was started orally on day 0, the day of arthritis induction, and continued for 7 days. Knee swelling was measured using digital calipers and expressed as a ratio of right (arthritic) vs left (control) knee swelling. The area under the curves (AUCs) of the treatment groups were then calculated as percentage inhibitions of the control vehicle treated animals.
- Compound 13E was tested against a panel of 262 kinases at 1 μ M and inhibited 14 human kinases with \geq 95%: CaMKII β , γ , δ ; CK1 γ ,2,3; DAPK1,2; Met; Mnk2; PDGFR α (D842V); Pim-1; PRAK; ULK2; ZIPK.